scientific reports

Check for updates

OPEN

Spatio-temporal variations and multi-scenario simulation of landscape ecological risk in the drylands of the Yellow River Basin

Jing Li[1], Shuai Li[2]✉, Xiaohui Wang[1], Guangfu Xu[2] & Jiacheng Pang[2]

Over the past decades, the drylands of the Yellow River Basin (YRBD) have undergone profound changes in landscape patterns and ecological dynamics, significantly impacting regional sustainable development. To assess the spatio-temporal variations of ecological risk in the YRBD and provide guidance for sustainable regional development, we constructed a coupled Land Use-Landscape Ecological Risk Model-Geographical Detector-PLUS framework for the assessment, analysis, and simulation of dryland landscape ecological risk (LER). The main findings are as follows: (1) Between 2000 and 2020, the area of built-up land, forest, grassland, and water in the YRBD increased, while the area of unused land and cropland decreased. (2) LER exhibited significant spatial heterogeneity, dominated by Sub-low and Low risks. High risk areas were primarily located in the western Inner Mongolia Plateau, whereas Low risk areas were prevalent in the Loess Plateau, with an overall decline in risk levels over the 20 years. (3) Water resources, ecological status, and human activities are the main driving factors affecting LER, with the impact of human activities becoming increasingly significant over the past 20 years. (4) Under three development scenarios in 2030, the LER is projected to further decrease, although the impact of these scenarios varies across different research sub-regions. Notably, the Ecological Priority Scenario emerges as more effective in mitigating regional LER. (5) Developing precise land use policies tailored to regional characteristics, continuously implementing ecological restoration projects, strengthening water resource management, and enhancing monitoring capabilities are effective ways to reduce LER in the YRBD. This study systematically quantified the impact of different development scenarios on LER in the YRBD, revealing its spatio-temporal characteristics, and emphasized the importance of planning guidance, ecological restoration, and risk monitoring to align regional development with ecological protection. The findings provide scientific evidence for ecological protection and sustainable development in the YRBD and other drylands, offering valuable insights for global dryland ecological risk management.

Keywords Yellow River Basin, Dryland, Landscape ecological risk, Geographical detector, Multi-scenario simulation, PLUS

Drylands account for approximately 40% of the terrestrial land surface and support more than one-third of the global population[1,2]. Despite being water-scarce and ecologically fragile, they provide critical ecosystem services including water formation, biodiversity maintenance, food production, and carbon storage[3,4]. However, multiple pressures, such as current irrational land use (LU), rapid urbanization, and demographic change[4], are causing significant alterations in the structure and function of dryland ecosystems. These pressures exacerbate land desertification, and make ecological risks increasingly salient[5–7]. According to the methods of the United Nations Convention to Combat Desertification (UNCCD), Wu et al.[8] revised the climatic zones of China, clearly defining the extent of drylands. These dryland are also recognized by Chinese authorities as potential extent of desertification[9,10].According to this delineation, drylands account for 47% of China's land area, and face a series of issues such as water scarcity, sparse vegetation, low land productivity, and severe desertification[2,11]. Therefore, ecological protection, restoration, and desertification control in these areas have been priorities in China's efforts. Over the past decades, due to population growth, economic development, and the implementation of a series

[1]Research Institute of Forestry Policy and Information, Chinese Academy of Forestry, Beijing 100091, China. [2]Inner Mongolia Dengkou Desert Ecosystem National Observation Research Station, Experimental Center of Desert Forestry, Chinese Academy of Forestry, Dengkou 015200, China. ✉email: lisshaxs@163.com

of ecological projects, the structure and function of ecosystems and LU patterns in drylands have undergone significant changes[12,13]. However, the specific impacts of these changes on regional ecology remain unclear, making ecological risk assessment in drylands urgently needed.

Ecological risk assessment has become an important tool for evaluating regional ecological environmental quality[14]. It has evolved from risk identification of microenvironmental factors such as pollution and heavy metals[15–18] to broader topics such as ecosystem and regional ecology. The scale of assessment has also shifted from micro to macro[19,20], emphasizing the intersection of geography and ecology and the spatial heterogeneity of geography[21,22]. Assessing ecological risk from a LU perspective at the landscape scale has become one of the most widely used methods[23]. This approach uses landscape pattern indices to describes the impact of human disturbance or natural change on the composition, structure, function, and processes of specific regional landscapes revealing the spatial impacts of landscapes on sources of risk[24–26], and the corresponding countermeasures. Existing research on landscape ecological risk (LER) assessment mainly focuses on areas with intensive human activities, such as watersheds[27–29], urban areas[30,31], wetlands and coastal regions[32,33], as well as key risk control areas like industrial and mining zones[34] and nature reserves[14]. However, studies on special ecologically fragile areas like drylands are relatively scarce. Additionally, recent studies mainly focus on quantitative analysis of landscape patterns or indirectly reflect LERs through analysis results, lacking quantitative analysis of driving factors.

The drylands of the Yellow River Basin (YRBD), located in northwestern China, hold a priority position in China's current and future policy planning for desertification control, biodiversity conservation, ecological conservation and high-quality development strategies[35,36]. The YRBD also exhibits significant spatial heterogeneity in terms of its topography, climate conditions, and socio-economic factors, making its ecological changes highly representative and typical for dryland regions in China and globally. With population growth, economic development, and the implementation of ecological projects[37] such as the Three North Shelter Forest Project, the Returning Farmland to Forests and Grasslands Project, the Beijing–Tianjin Sandstorm Source Control Project, the Natural Forest Protection Project, and the Returning Grazing Land to Grassland Program, the LU and landscape patterns in this typical dryland region have undergone significant changes. This makes it an ideal example for studying LER in drylands. However, current research on ecological risks in the YRBD is mostly concentrated in specific counties and cities[38–40], lacking systematic studies on LERs and their trends at the regional scale, as well as in-depth exploration of driving mechanisms and future LU policies. Therefore, conducting a comprehensive study on the overall LER of the YRBD at a regional scale is not only of significant academic value but also provides scientific evidence for policy-making[41,42].

This study selects the YRBD as the study area and uses the LER assessment method on a large scale to assess and predict ecological risk changes in this typical dryland over the past 30 years and into the future, with a quantitative analysis of driving factors. Through this study on LER in typical drylands, we aim to (1) analyze the LU change pattern in the YRBD over the past 20 years; (2) explore the spatio-temporal variations and driving factors of LER based on LU change; and (3) assess the changes of LER in the YRBD under various future development scenarios to provide guidance for future LU policy-making. This research will contribute to a comprehensive understanding of LERs and their trends in the YRBD, providing scientific evidence for formulating reasonable ecological protection and LU policies for the study area, China, and even dryland regions globally.

Results

LU changes

The spatial distribution and alterations of LU in the YRBD between 2000 and 2020 are displayed in Fig. 1. Overall, unused land, grassland and cropland dominate the YRBD. Taking 2020 as an example, grassland, unused land and cropland together accounted for 88.23% of the entire study region (Fig. 1d). Between 2000 and 2020, although different LU types exhibited diverse degrees of alterations, the spatial distribution and structural features of LU types remained consistent. During the study period, the regions of water, grassland, forest and built-up land demonstrated an increasing trend, whereas those of cropland and unused land showed an opposite trend.

Combining the changes in LU quantity (Fig. 1d) and transfer matrix (Table 1), it is noted that built-up land is the LU type with the most dramatic growth and change in the study region. Notably, over two decades, there has been a significant increase of 60.87%, equivalent to 5790 km^2, mainly transferred from cropland, grassland, and unused land. The forest also grew rapidly, with an increase of 12.73% (3333 km^2) over 20 years, accompanied by a decrease in grassland and cropland areas. Throughout the experimental period, grassland transferred the largest area to other land classes, with a total transfer of 17,316 km^2. Although the grassland area increased by 0.38% (1883 km^2) over 20 years, it exhibited a declining trend in the past decade. With the increases in the areas of built-up land, forest, and water, the areas of cropland and unused land were reduced by 5.71% (7431 km^2) and 2.59% (4743 km^2), respectively, over 20 years.

Spatio-temporal variation of LER

Spatial distribution of the LER

The spatial distribution of LER in the YRBD in 2000, 2010, and 2020 are displayed in Fig. 2a–c. The LER in the study region exhibits obvious spatial heterogeneity. Considering the spatial heterogeneity of altitude, topography and LU, the YRBD are further assigned to three subregions: the Tibetan Plateau (TP), the Inner Mongolia Plateau (IMP) and the Loess Plateau (LP), for the analysis of LER variations.

Based on the mean value change in the ERI (Fig. 2d), the overall LER in the study region and each subregion has steadily reduced over the past two decades. In terms of the average value of ERI in different subregions, the IMP has the highest risk, followed by the TP, and the LP has the lowest risk. Throughout the experimental

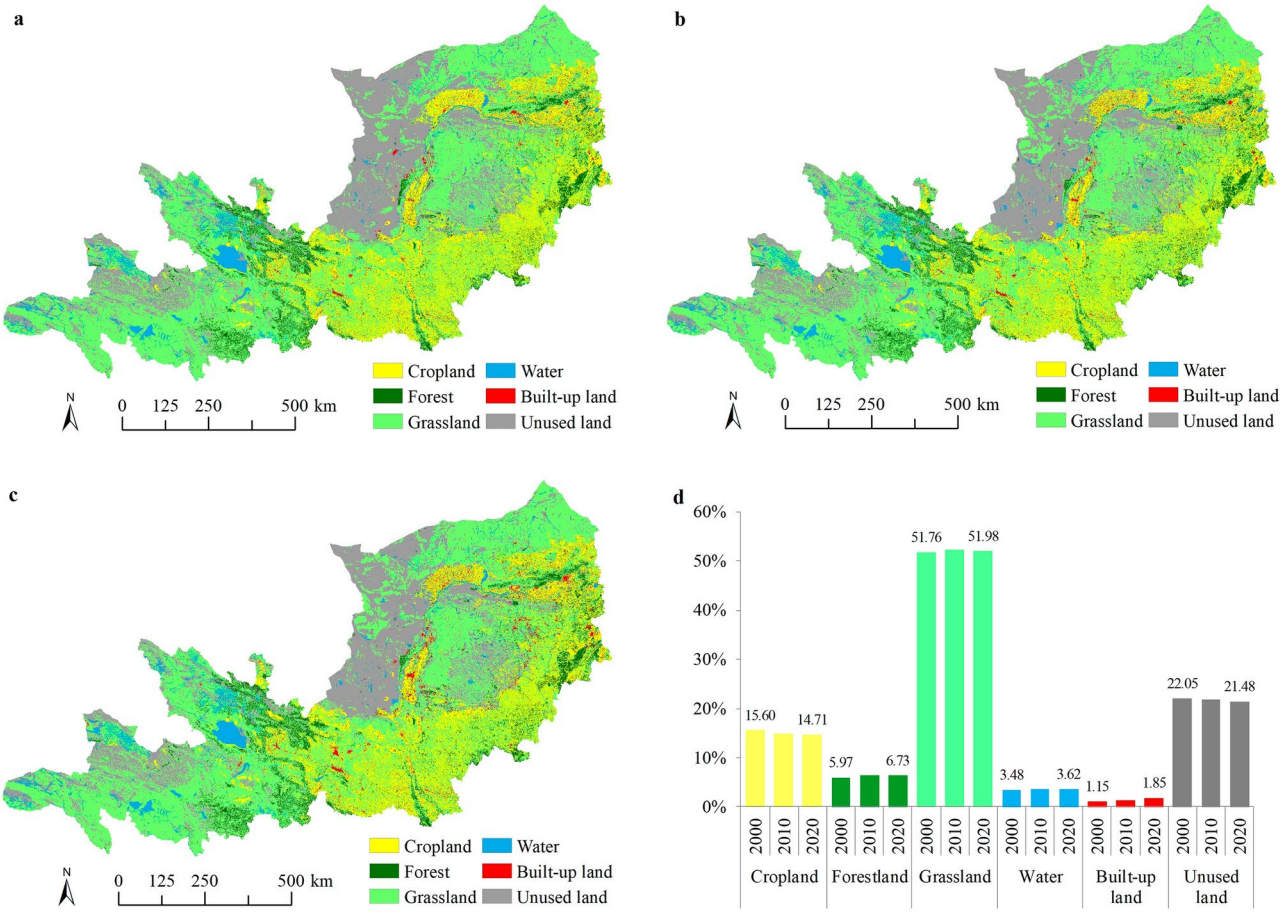

Fig. 1. Land use maps in 2000 (**a**), 2010 (**b**), 2020 (**c**), and percentages of Land use types between 2000 and 2020 (**d**). (Software: ArcMap 10.6, http://www.esri.com).

LU types	Area of land in 2020						
	Cropland	Forest	Grassland	Water	Built-up land	Unused land	Total area of lost
Area of land in 2000							
Cropland	117,390	2111	6202	450	2728	1052	12,543
Forest	361	48,185	645	77	316	176	1575
Grassland	3470	2183	413,838	1223	2887	7553	17,316
Water	372	62	556	27,290	144	520	1654
Built-up land	275	78	351	33	8509	345	1082
Unused land	634	474	11,445	1039	797	169,267	14,389
Total area of added	5112	4908	19,199	2822	6872	9646	

Table 1. Transfer matrix for the diverse Land use types between 2000 and 2020 (km^2).

period, the LER levels were mainly Low and Sub-low, primarily distributed in the eastern TP, eastern IMP and most of the LP. The High risk and Sub-high risk regions are mostly found in the western part of the IMP. The Middle risk regions are mostly found in the western TP and the central and northeastern parts of the IMP.

From the changes in LER levels from 2000 to 2020 (Table 2), the proportion of Low risk regions has continuously risen, whereas that of Sub-low risk regions has reduced. The proportion of Middle risk areas has fluctuated, while the proportions of Sub-high and High risk regions have continuously reduced. With respect to regional changes, the proportion of Low risk areas in the TP has continuously increased over the past two decades, while the proportions of Sub-low and Middle risk regions have slightly decreased. The alterations in different LER levels in the IMP were consistent with the overall trend of the study region. The proportion of Low and Sub-low risk regions in the LP also follows the overall trend of the study area over the past two decades, while Middle, Sub-high and High risk regions remained largely unchanged.

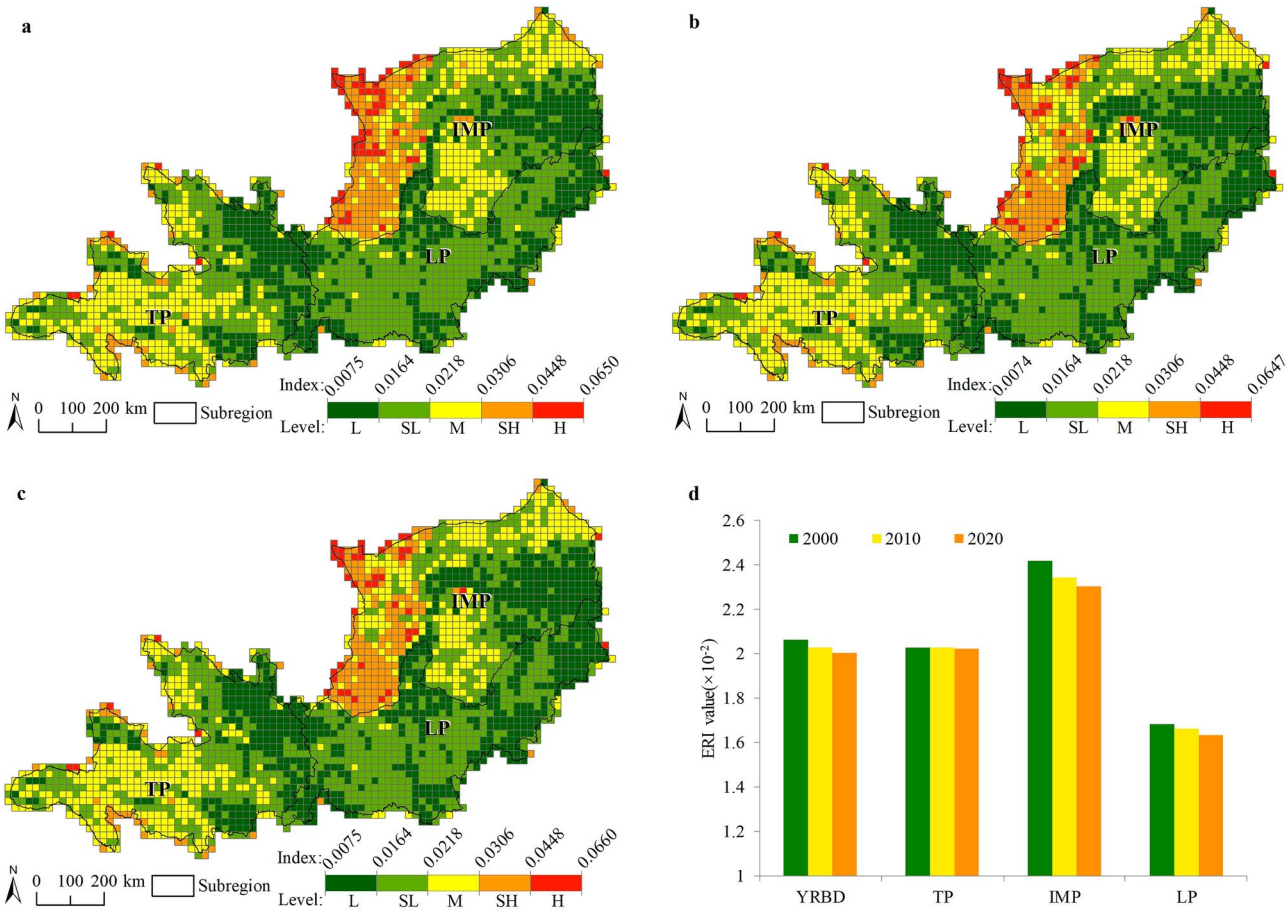

Fig. 2. Spatial pattern of landscape ecological risk in 2000 (**a**), 2010 (**b**), 2020 (**c**) and the mean value of landscape ecological risk index (ERI) in different regions (**d**) (Software: ArcMap 10.6, http://www.esri.com). *Notes*: Low (L), Sub-low (SL), Middle (M), Sub-high (SH), High (H); The drylands of the Yellow River Basin (YRBD), the Tibetan Plateau (TP), the Inner Mongolia Plateau (IMP) and the Loess Plateau (LP).

Region	Year	Low risk	Sub-Low risk	Middle risk	Sub-high risk	High risk
YRBD	2000	31.30	40.65	19.57	6.80	1.67
	2010	33.90	38.44	20.17	6.02	1.48
	2020	35.87	37.28	19.54	6.00	1.30
TP	2000	28.30	40.20	30.03	1.45	0.02
	2010	28.35	40.01	30.18	1.45	0.02
	2020	29.01	39.94	29.58	1.45	0.02
IMP	2000	23.24	30.18	25.28	16.84	4.45
	2010	25.51	29.11	26.77	14.68	3.94
	2020	27.18	29.10	25.62	14.64	3.47
LP	2000	44.66	54.21	0.98	0.15	0.00
	2010	50.45	48.35	0.96	0.24	0.00
	2020	54.24	44.56	0.96	0.24	0.00

Table 2. Percentage distribution of landscape ecological risk in the drylands of the Yellow River Basin between 2000 and 2020 (%). The drylands of the Yellow River Basin (YRBD), the Tibetan Plateau (TP), the Inner Mongolia Plateau (IMP) and the Loess Plateau (LP).

Spatio-temporal variations of the LER

As shown in Fig. 3a, the risk units of LER reduction and increase in the YRBD from 2000 to 2010 were distributed separately in the IMP and the LP, with the TP mainly remaining unchanged. Overall, the study area exhibited a greater improvement in landscape ecology conditions than deterioration. Within the 2010–2020 period

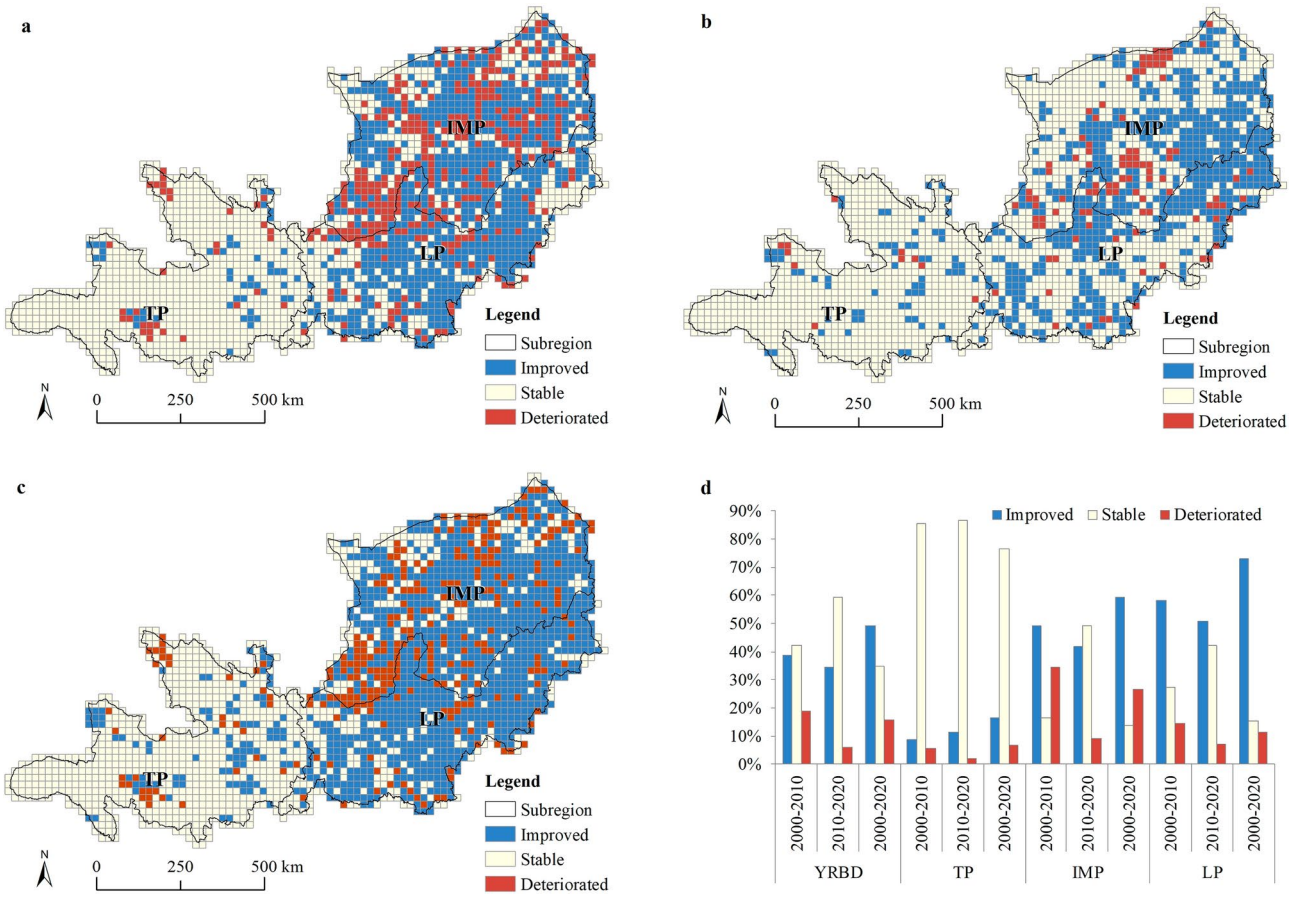

Fig. 3. Spatial pattern of landscape ecological risk changes from 2000 to 2010 (**a**), 2010 to 2020 (**b**), 2000 to 2020 (**c**) and the percentage of area for each landscape ecological risk change class in different regions (**d**) (Software: ArcMap 10.6, http://www.esri.com). Notes: The drylands of the Yellow River Basin (YRBD), the Tibetan Plateau (TP), the Inner Mongolia Plateau (IMP) and the Loess Plateau (LP).

(Fig. 3b), the units of increased LER declined substantially, with the proportion of landscape ecology recovery or stability reaching 93.81% (Fig. 3d). Over time, there has been an obvious decrease in LER in the study region (Fig. 3c), indicating an overall improvement in landscape ecology conditions.

From the subregional perspective (Fig. 3d), the proportion of units with decreased LER in the TP gradually increased over the two periods from 2000 to 2020, with 16.55% of units with improved landscape ecology conditions and 6.73% with deteriorated conditions. In the IMP, approximately 86.18% of units experienced changes in LER between 2000 and 2020. Notably, the proportion of units with improved landscape ecology conditions was 59.34%, the proportion of units with deteriorated was 26.85%, and only 13.82% of units remained stable. The landscape ecology conditions in the LP also showed a predominant improvement, accounting for 73.14%. Overall, during the 2000–2020 period, the proportion of units with stable landscape ecology conditions was predominant on the TP, while the proportion of units with improvement was predominant on the IMP and the LP, with the LP having a higher proportion of units with improved landscape ecology conditions than the IMP.

Spatial autocorrelation analysis

The global spatial autocorrelation Moran's *I* of LER in the YRBD in 2000, 2010, and 2020 were 0.7266, 0.6773 and 0.6827, respectively. The LER exhibited significant positive spatial autocorrelation ($p < 0.01$) and demonstrated spatial clustering throughout the region (Fig. 4). From 2000 to 2010, the Moran's *I* value decreased, and there was a slight increase from 2010 to 2020, implying a decreasing trend in the spatial clustering and a reduction in spatial autocorrelation of LER.

The local spatial autocorrelation result (Fig. 5) showed that the High-High clusters were mostly found in the western part of the IMP and sporadically distributed in the eastern part of the TP, where the primary LU type was desert. The Low–Low clusters were distributed at the junction of the TP and the LP, as well as in the eastern part of the IMP and the LP, where the main LU types were cropland and forest. In terms of spatial changes, the High–High clusters continuously decreased over time, while the Low–Low clusters increased. Additionally, Low–High outliers were observed near the High–High clusters, where the LU types were mainly grassland and cropland surrounding the desert, which were prone to be converted into High risk regions. In the LP and the

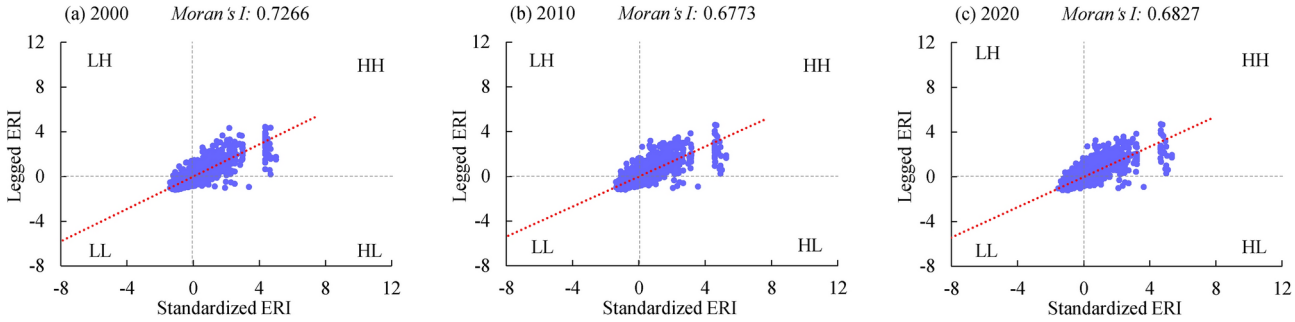

Fig. 4. Moran's *I* scatter plot of landscape ecological risk in 2000 (**a**), 2010 (**b**) and 2020 (**c**) (Software: GeoDa 1.20.0.36, https://geodacenter.github.io/).

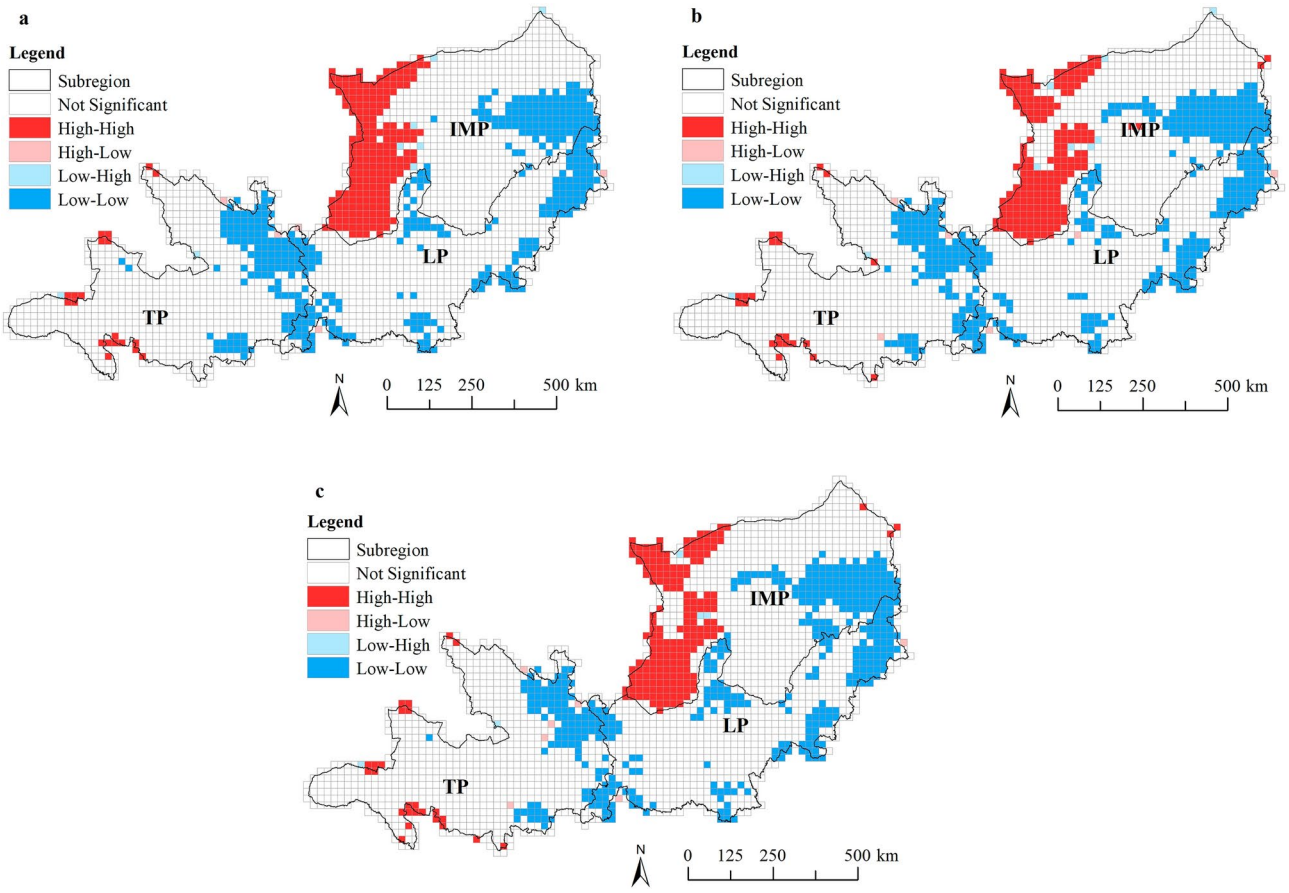

Fig. 5. Spatial Lisa cluster of landscape ecological risk in 2000 (**a**), 2010 (**b**) and 2020 (**c**) (Software: ArcMap 10.6, http://www.esri.com). *Notes*: The Tibetan Plateau (TP), the Inner Mongolia Plateau (IMP) and the Loess Plateau (LP).

eastern part of the TP, there were also a few High–Low outliers near the Low–Low clusters, where the LU types were grassland surrounding forest or cropland.

Simulation of future variation of LER

Simulation of LU under multiple scenarios

The LU patterns and predicted data of the YRBD under multiple scenarios in 2030 simulated by the PLUS model are displayed in Fig. 6 and Table 3, respectively. The simulation results indicate that, compared with 2020, there are different trends in LU types under the three scenarios. Under the Natural Development Scenario (NDS), the LU types continue the trends observed from 2010 to 2020, with increases in forest, water, and built-up land, as well as decreases in cropland, grassland, and unused land. Among them, the unused land and grassland decrease the most, by 2219 km^2 and 2097 km^2 respectively. The region of built-up land increases significantly by

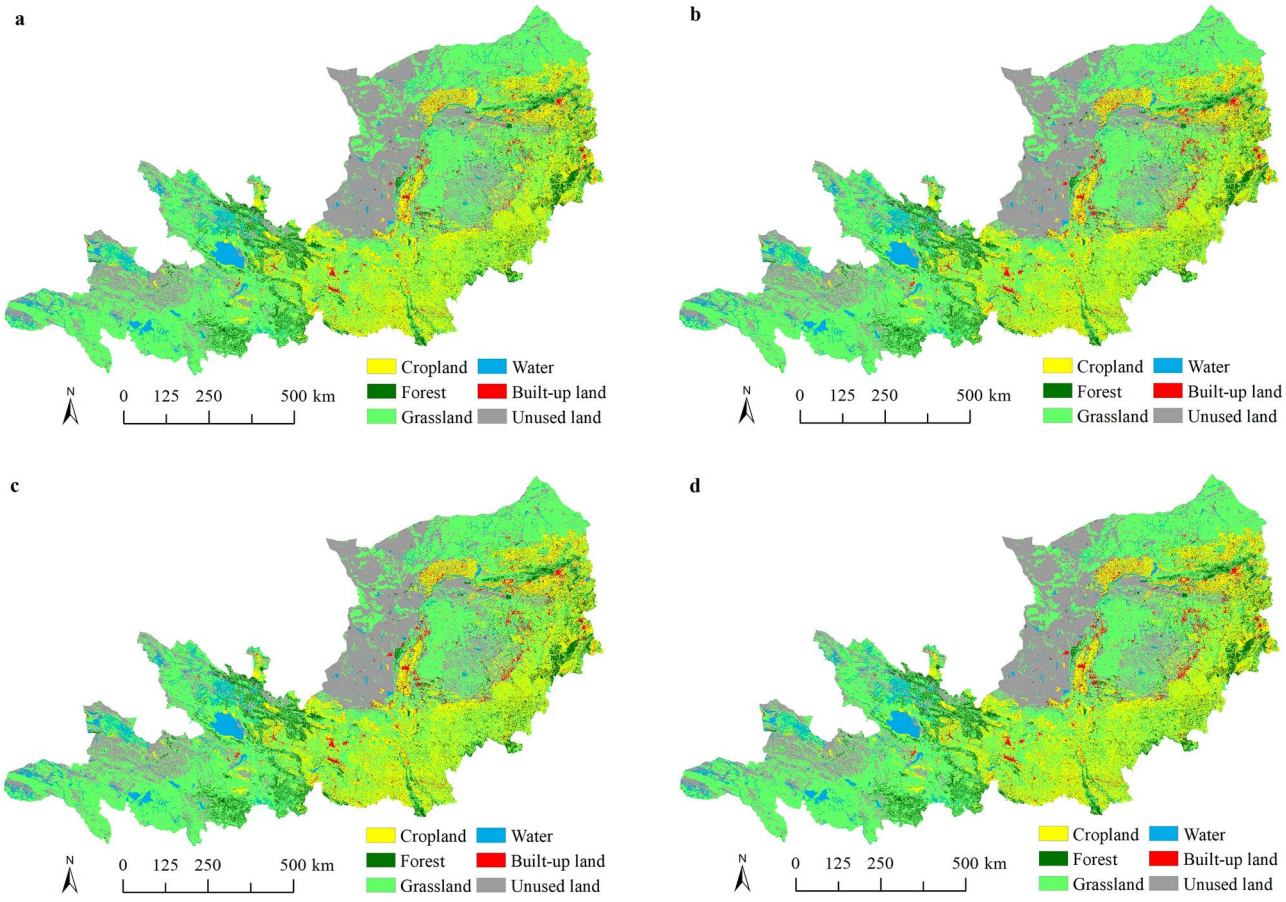

Fig. 6. Land use maps in 2020 (**a**), Natural Development Scenario (NDS, **b**), Ecological Priority Scenario (EPS, **c**) and Cropland Protection Scenario (CPS, **d**) (Software: ArcMap 10.6, http://www.esri.com).

Year	Scenarios	Cropland	Forestland	Grassland	Water	Built-up land	Unused land
2020		122,502	53,093	433,037	30,112	15,381	178,913
2030	NDS	121,384	53,304	430,940	30,561	20,155	176,694
	EPS	122,210	53,451	431,509	30,701	18,748	176,419
	CPS	122,767	53,169	430,628	30,456	19,346	176,672
2020–2030	NDS	−1118	211	−2097	449	4774	−2219
2020–2030	EPS	−292	358	−1528	589	3367	−2494
2020–2030	CPS	265	76	−2409	344	3965	−2241

Table 3. Regions of different land use types in 2030 under three scenarios and the area of change compared with 2020 (km^2).

4774 km^2. Under the Ecological Priority Scenario (EPS), the regions of forest, water and built-up land continue to increase, by 358 km^2, 589 km^2 and 3367 km^2 respectively, whereas those of cropland, grassland, and unused land decline, by 292 km^2, 1528 km^2 and 2494 km^2 respectively. Under the Cropland Protection Scenario (CPS), except for an increase of 265 km^2 in cropland, the trends in other LU types are similar to those under the NDS and EPS, with forest, water and built-up land areas increasing and grassland and unused land decreasing.

Comparing the multiple scenarios, the increase in production land(cropland), living land (built-up land), and ecological land (forest and water) in the YRBD mainly comes from grassland and unused land. The cropland area decreases the most under the NDS, slightly decreases under the EPS, and slightly increases under the CPS. The forest and water increase under all scenarios, with the largest increase under the EPS and the smallest increase under the CPS. The grassland area decreases significantly in all scenarios, with the largest decrease under the CPS and the smallest decrease under the EPS. Built-up land undergoes the most drastic changes among the LU types under all scenarios, with the largest increase under the NDS and the smallest increase under the EPS. The area of unused land decreases significantly under all scenarios, with the largest decrease under the EPS.

Spatio-temporal variation of LER under multiple scenarios

To reveal the variations of LER in the YRBD under multiple scenarios, the LER for the year 2030 was predicted. The results are shown in Fig. 7. The spatial distribution patterns of different levels of LER are relatively similar to those of 2020. High risk and Sub-high risk regions are still primarily found in the western IMP. Middle risk regions are primarily found in the central part of the TP as well as the western, northern and central parts of the IMP. Meanwhile, Sub-low and Low risk areas are primarily found in the eastern TP, eastern IMP and most of the LP. With regard to spatial variations, the Low risk areas have expanded under all scenarios, compared with those of 2020. The expansion is mainly located in the western and southern parts of the TP, southern IMP and central LP. Correspondingly, an obvious decline is observed in Sub-low risk and Middle risk regions, whereas the changes in Sub-high and High risk regions are not significant.

In terms of the mean values of the ERI under multiple scenarios (Fig. 7d), it can be observed that the mean values of ERI have decreased in both the overall study area and subregions in 2030, as compared with those of 2020, across all scenarios. Notably, the EPS exhibits the largest decrease in the mean value of ERI in both the overall study area and the TP region, followed by the NDS and the CPS. Conversely, in the IMP and LP regions, the NDS demonstrates the largest decrease in the mean value of ERI, followed by the EPS and the CPS.

From the variations in the LER levels of multiple scenarios in 2030 (Table 4), compared with 2020, the proportion of Low risk regions in the overall study has significantly elevated, while the proportions of Sub-low, Middle, and High risk regions have markedly decreased. However, the proportion of Sub-high risk areas has shown a slight decrease in the EPS, no change in the NDS and an increase in the CPS. Comparing multiple scenarios, the EPS has the highest total proportion of Low and Sub-low risk regions, reaching 73.50%, followed by the NDS and the CPS, which are 73.44% and 73.35% respectively. The EPS has the smallest total proportion of Mand Sub-high risk regions (19.25% and 5.99% respectively), followed by the NDS (19.30% and 6.00%, respectively) and the CPS (19.35% and 6.05%, respectively). The proportions of High risk regions are the same for all three scenarios.

Compared to 2020, the LER in each subregion has decreased under the three scenarios. In the TP, all three scenarios exhibit a significant increase in Low and Sub-low risk regions, while experiencing a notable decrease

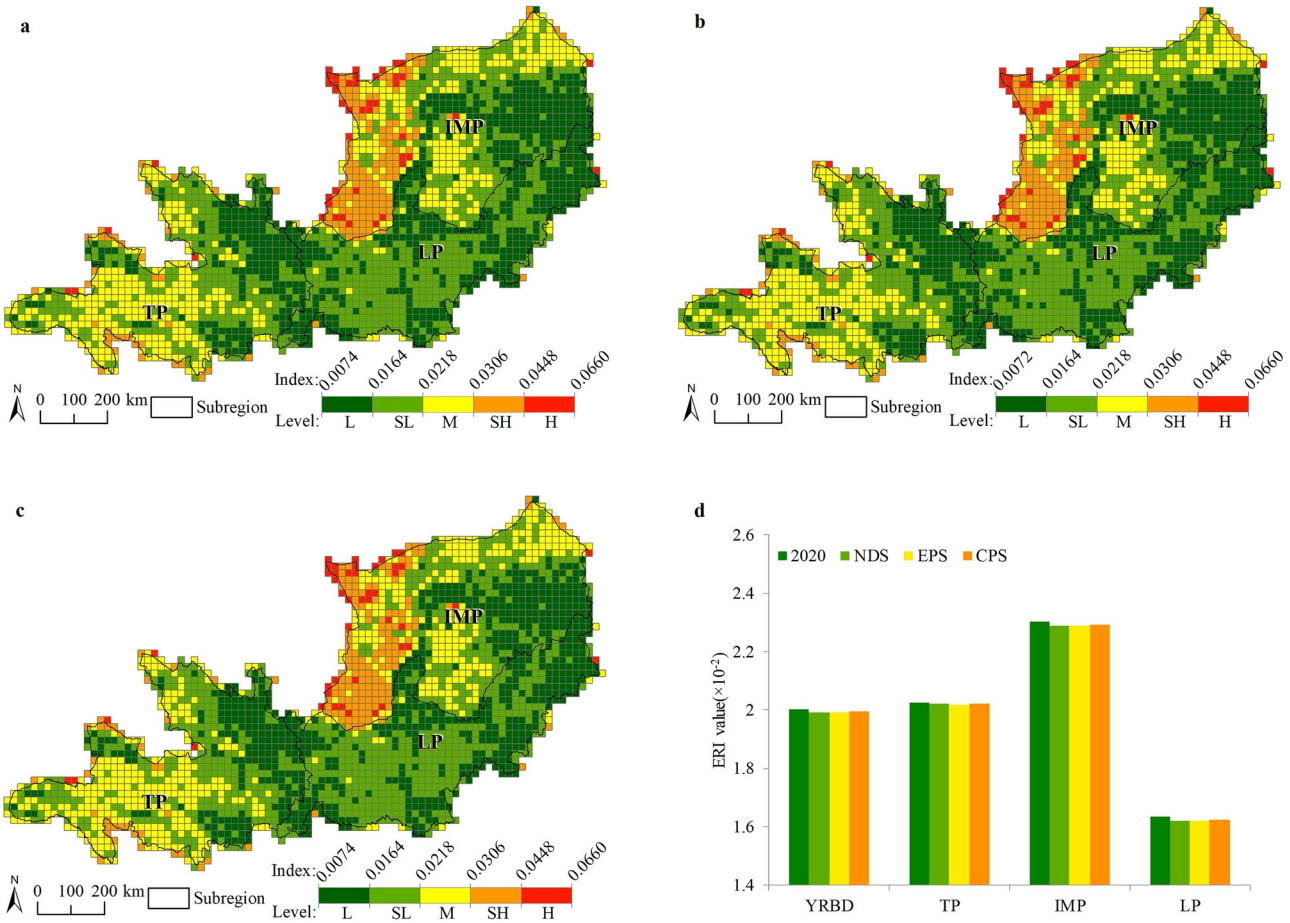

Fig. 7. Spatial pattern of landscape ecological risk in Natural Development Scenario (NDS, **a**), Ecological Priority Scenario (EPS, **b**), Cropland Protection Scenario (CPS, **c**) and the mean values of landscape ecological risk index (ERI) in different regions (**d**) (Software: ArcMap 10.6, http://www.esri.com). *Notes*: Low (L), Sub-low (SL), Middle (M), Sub-high (SH), High (H); The drylands of the Yellow River Basin (YRBD), the Tibetan Plateau (TP), the Inner Mongolia Plateau (IMP) and the Loess Plateau (LP).

Region	Year	Low risk	Sub-low risk	Middle risk	Sub-high risk	High risk
YRBD	2020	35.87	37.28	19.54	6.00	1.30
	NDS	36.80	36.64	19.30	6.00	1.26
	EPS	36.89	36.61	19.25	5.99	1.26
	CPS	37.02	36.33	19.35	6.05	1.26
TP	2020	29.01	39.94	29.58	1.45	0.02
	NDS	29.56	39.39	29.58	1.45	0.02
	EPS	29.30	39.95	29.32	1.41	0.02
	CPS	29.45	39.69	29.39	1.45	0.02
IMP	2020	27.18	29.10	25.62	14.64	3.47
	NDS	27.87	29.17	24.98	14.64	3.34
	EPS	28.09	28.87	25.06	14.64	3.34
	CPS	28.33	28.31	25.26	14.76	3.34
LP	2020	54.24	44.56	0.96	0.24	0.00
	NDS	55.88	42.93	0.95	0.24	0.00
	EPS	56.18	42.61	0.96	0.24	0.00
	CPS	56.16	42.63	0.96	0.24	0.00

Table 4. Percentage distribution of landscape ecological risk in the drylands of the Yellow River Basin between 2020 and 2030 (%). The drylands of the Yellow River Basin (YRBD), the Tibetan Plateau (TP), the Inner Mongolia Plateau (IMP) and the Loess Plateau (LP).

in Middle risk, Sub-high risk, and High risk regions. Among the three scenarios, the EPS demonstrates the most significant changes, with the highest increase in the overall proportion of Low and Sub-low risk regions (0.30%), as well as the most significant decline in Middle and Sub-high risk regions (0.26% and 0.04%, respectively). High risk regions remain unchanged. In the IMP, the LER under the three scenarios displays an increase in Low and Sub-low risk regions, along with a decrease in Middle, Sub-high, and High risk regions. The NDS exhibits the most significant changes, with an increase in both Low and Sub-low risk regions, and the highest increase in their combined proportion. The decline in Middle and High risk regions are also the most pronounced. There have been slight changes in the LP, characterized by an increase in Low risk regions and a decline in the Sub-low risk regions. Collectively, the EPS shows the most substantial increase in Low risk regions in the LP.

Discussion

Causes of LU change

The spatial distribution of LU in the YRBD exhibit significant spatial heterogeneity (Fig. 1). In the TP, due to uneven precipitation and high-cold climate characteristics[43], the source region of Yellow River is dominated by grassland, while the north of the source region is characterized by unused land (desert). Most of the IMP belongs to arid and semi-arid areas, where the limited precipitation results in the region being mainly covered by unused land and grassland. Forest are mainly found in mountainous areas due to the influence of terrain undulation and altitude. These areas often create microclimatic environments distinct from the surrounding dryland regions, providing suitable conditions for forest formation[44]. The distribution of cropland in the YRBD is mainly of two types: irrigated cropland concentrated in the plains along the Yellow River, and rainfed cropland widely distributed in the hilly regions of the LP. This distribution is primarily due to the different topographical features and water resource utilization in the YRBD. Additionally, built-up land (urban and industrial) is mainly distributed in the plains and river valley areas. Water also shows significant spatial heterogeneity, with most water concentrated in the TP and a few found in the desert areas of the IMP.

During the period from 2000 to 2020, significant changes occurred in different LU types in the YRBD. Population growth and rapid economic development led to increased demand for urban and industrial land, resulting in a substantial increase in built-up land, primarily converted from cropland, grassland, and unused land (Table 1). This transformation is consistent with other studies of urban expansion in the study area[45,46]. Liu et al. studied the LU changes in Lanzhou City over the past 20 years and found that significant urban expansion led to a reduction in cropland, forest, and grassland, with significant reduction in cropland[45]. Wei et al. also found that the urban expansion in the Hohhot–Baotou–Ordos–Yulin urban agglomeration mainly occupied unused land, grassland, and cropland[46].

Over the past 20 years, the increase in forest and grassland and the decrease in unused land in the YRBD have mainly benefited from the implementation of ecological projects such as the Three North Shelter Forest Project, the Returning Farmland to Forests and Grasslands Project, and the Returning Grazing Land to Grassland Program[43,47]. These projects comprehensively consider desertification control, soil erosion reduction, and ecosystem quality improvement, significantly increasing vegetation coverage in the project areas[48]. The transfer matrix (Table 1) also shows that the increase in forest mainly comes from cropland and grassland, the increase in grassland mainly from unused land, while unused land mainly transfers to cropland and grassland. These changes are consistent with the research results of Fu et al.[49]and Liao et al.[50], further clarifying the effectiveness of ecological projects implemented in the YRBD. This deepens the understanding of the reasons for LU change and

confirms the importance of balancing land management strategies between development and conservation. It also proves the significant success of the ecological projects implemented in the YRBD. Moreover, we also found that the area of water has continuously increased during the study period (Fig. 1), with changes occurring mainly in the TP. This change has been confirmed to be related to glacier melting caused by rising temperatures[51,52].

Spatio-temporal patterns of LER

The spatial pattern of LER in the YRBD shows a clear spatial differentiation. This pattern is consistent with the findings of Liu et al.[53] and Hua et al. [54] on LER in the Yellow River Basin and specific sections within the basin. The LER of the study area is closely related to the distribution of LU types. Regions dominated by unused land have higher LER, while those dominated by forest, cropland, and grassland have relatively lower LER. This distribution pattern reflects the importance of LU management in regional ecological risk management[55]. During the period from 2000 to 2020, the overall LER in the study area shows a declining trend. This trend is closely related to the series of ecological projects implemented by the Chinese government in the region since the late 1970s. These projects have effectively increased vegetation coverage, reduced unused land, improved the overall quality of the ecological environment[48,56], and mitigating LER[57].

We also found that the patterns of LER variation in the TP, IMP, and LP are different. In the TP, climate warming and humidification, along with strict land management policies, have enhanced ecosystem quality and functionality[58]. Additionally, due to minimal human interference, LU changes are minor, resulting in a predominantly stable LER, with some declines. In the IMP, the central and eastern regions have seen significant vegetation improvement due to largescale national land greening projects. However, the western region, with a more fragile ecological environment, has not experienced significant vegetation improvement, resulting in a pattern of primarily decreasing but also some increasing LER. The LP has benefited from extensive ecological restoration projects and favorable natural conditions, significantly increasing vegetation coverage and substantially reducing regional LER. These changes reflect the differences in natural conditions and management policies among the different sub-regions. The TP benefits from ecological protection policies focusing on natural recovery, the IMP relies on large-scale vegetation protection and afforestation projects, while the LP has significantly improved its ecological environment through comprehensive ecological protection and restoration projects. Under the combined influence of these factors, the LER in the YRBD shows an overall declining trend.

The influence of driving factors on LER

The Geographical Detector Model (GDM) was utilized to quantitatively identify the main factors influencing the spatial pattern of LER in the YRBD from three dimensions: natural geography, ecological status, and socio-economic factors (as show in Table 5). The results indicate that the most significant influencing factor is the distance to water, with an average q value of 0.35. This is followed by NDVI (Normalized Difference Vegetation Index, 0.29), annual mean precipitation (0.27), NPP (The Net Primary Productivity, 0.27), and the distance to residence (0.27), while the mean values of other factors are all below 0.1. This reveals that natural geography conditions, vegetation status, and human activities jointly determine the spatial pattern of LER in the study area, with water resources playing the most critical role. This is mainly because water resources are the most important factors affecting vegetation distribution patterns and ecosystem quality in dryland regions[59,60]. Zhang et al. also confirmed that ecological vulnerability in the arid regions of northwest China is largely influenced by the distribution of natural water resources[61].

Analyzing the changes in q values of various driving factors over the study period, we found that changes in NDVI and NPP are the main reasons for the reduction of LER in the YRBD (q values increased from 0.24 and 0.25 to 0.33 and 0.28, respectively). This is consistent with the findings of Zhu et al.[62] and Wang et al.[63], which attribute the results to the implementation of a series of ecological projects such as the Three-North Shelter Forest Program and the Grain for Green Project. These projects have gradually improved regional vegetation conditions and ecosystem functions, with the cumulative effects of ecological restoration becoming increasingly evident, playing a significant role in reducing ecological risks[64]. Moreover, as the overall LER in the arid areas of the Yellow River Basin decreased, the q values of natural geographical indicators such as distance to water, annual precipitation, and annual mean temperature also decreased. Notably, the q value of the most significant influencing factor, distance to water, decreased from 0.41 in 2000 to 0.32 in 2020. This may be due to the enhanced water conservation capacity brought about by improved vegetation and ecological quality, thereby reducing the constraint of moisture on ecological risks[65].

The changes in distance to residence and population density reflect that the impact of socio-economic factors related to human disturbance on LER is gradually weakening. It is worth noting that the q value of GDP increased from 0.01 to 0.05 over the past 20 years, indicating that economic development in drylands is not contradictory to reducing LER. Economic development can promote environmental protection and ecosystem restoration

Year	DEM	Relief degree of surface	Annual mean temperature	Annual mean precipitation	NPP	NDVI	Distance to water	Distance to residence	Population density	GDP
2000	0.07	0.10	0.08	0.28	0.25	0.24	0.41	0.28	0.11	0.01
2010	0.07	0.09	0.06	0.28	0.27	0.30	0.32	0.26	0.10	0.05
2020	0.06	0.09	0.06	0.26	0.28	0.33	0.32	0.27	0.08	0.05
Mean	0.07	0.09	0.07	0.27	0.27	0.29	0.35	0.27	0.10	0.04

Table 5. The q-value of driving factors influencing spatial distribution of landscape ecological risk.

through technological innovation and effective utilization of ecological capital[66], providing new evidence for the coordinated development of ecology and economy in ecologically fragile areas.

Overall, the spatio-temporal variation in LER in the study area are driven by multiple factors, including natural geography, ecological status, and human activities. This study, based on GDM, quantitatively clarifies the dominant driving factors affecting the LER pattern, highlighting the critical roles of water resources, ecological restoration, and human activities. These results not only complement previous research but also provide theoretical support for more precise formulation of regional ecological protection and restoration strategies.

Choices for future scenarios and policy recommendations

From the perspective of overall LER changes, the spatial distribution pattern of LER under the three future scenarios is basically the same as in 2020, with the mean values for the entire study area and sub-regions in 2030 showing a decrease compared to 2020. However, the changes under different scenarios vary in the different sub-regions. The EPS shows the largest decrease in the mean LER values for the entire study area and the TP region, followed by the NDS and the CPS. In the IMP and LP, the NDS exhibits the largest decrease in mean LER values, while the decreases in the EPS and CPS are relatively smaller. Additionally, the areas of different risk levels show varying changes between the three scenarios. Overall, the EPS performs better in reducing the overall regional LER compared to the NDS and the CPS, but it also highlights that a single development model cannot meet the need to minimize ecological risk in different sub-regions.

When making development plans, it is necessary to choose appropriate development paths based on the conditions of different sub-regions, maximizing the balance between economic, social, and ecological factors to achieve the unity of ecological protection and economic development. The EPS has excellent performance in reducing LER but may limit economic development, requiring the use of innovative policy tools and scientific management strategies to balance economic benefits and ecological effects. The NDS, based on historical development trends, emphasizes the use of natural resources and locational advantages, offering economic development benefits but potentially bringing higher ecological risks, especially in ecologically fragile areas. Therefore, it is essential to establish stricter regulatory mechanisms to minimize environmental impacts, while enhancing public environmental education and community involvement. The CPS focuses on agricultural production and food security but may face conflicts between agricultural land and other LU types. Thus, this scenario requires a balance between agricultural production, economic development, and ecological protection.

By formulating scientifically LU planning and related policies, regional LER can be effectively reduce while promoting economic growth and improving livelihoods. Although the YRBD exhibit significant heterogeneity in terms of topography, ecological status, and climatic conditions, these heterogeneous areas are inseparable from the Yellow River flowing through them and form an integral whole. Therefore, it is necessary to strengthen the overall planning of the territorial space in the entire YRBD, rationally determine the layout of functional zones, and scientifically allocate ecological, living, and production spaces to minimize the adverse impacts of economic and social development on the ecological environment[63]. At the same time, it is crucial to continue promoting ecological protection and restoration projects, implementing and advocating for Nature-based Solutions to enhance ecosystem quality and service functions. Only by systematic promotion of measures such as scientific policy guidance, rational spatial planning and new technological applications can we truly achieve the coordination development of the economy, society, and environment in the YRBD, thereby effectively preventing and reducing LER.

Limitations and future perspectives

This study assesses the LER in the YRBD, providing a basis for the formulation of effective ecological management measures. However, there are several limitations. Firstly, due to the influence of spatial scale, the landscape pattern indices used in the assessment units of 20 km × 20 km[67] may overlook the LER conditions in certain areas. Secondly, in the calculation of landscape risk indices, we directly assigned landscape vulnerability values to different LU types. Although this method is widely used, it cannot reflect the spatial heterogeneity of different LU types[22,31], which is an issue that needs to be addressed in future research. Additionally, the study employs the PLUS model to simulate future LU patterns. While this model has certain advantages[32], it is still constrained by the accuracy of LU data and the selection of driving factors, resulting in uncertainties in simulating future LU changes and affecting the accuracy of LER assessments. Considering the temporal continuity of LU changes, this study selected three years to assess LER. However, these selected years do not allow for long-term continuous sequence analysis to explore spatio-temporal variations.

Future research should focus on several aspects. Firstly, optimizing LER methods from the perspective of evaluation index systems and index calculations. Secondly, improving the spatial and temporal accuracy of LU data and optimizing the selection of driving factors to comprehensively capture the multi-scale variation characteristics of LER. Thirdly, implementing long-term LER monitoring and continuous scenario analysis to provide real-time references for updating and optimizing protection strategies and LU planning. Through these in-depth studies, it will be more helpful to understand the dynamic changes in LER in drylands, provide scientific evidence for regional ecological protection and sustainable development, and offer important insights for ecological protection practices in other drylands regions worldwide.

Conclusions

This study takes the YRBD, a representative dryland region, as an example to analyze LU changes over the past 20 years. It explores the spatio-temporal changes and driving factors of LER from a landscape pattern perspective and predicts ecological risk under different development scenarios by simulating future land use patterns. The main conclusions are as follows: (1) From 2000 to 2020, LU types in the YRBD underwent significant changes. Built-up land, forest, and grassland increased, while unused land decreased. Built-up land significantly increased

by 60.87%, forest increased by 12.73%, and grassland areas also increased overall. These changes are mainly attributed to the implementation of a series of ecological projects. (2) The LER in the YRBD exhibits significant spatial heterogeneity, with High risk and Sub-high risk areas mainly concentrated in the western regions of the IMP. Over the past 20 years, the overall trend of LER has been decreasing, indicating an improvement in landscape ecological conditions. The reduction in LER is closely related to increased vegetation coverage, water resource management, and the implementation of various ecological projects. (3) LER shows significant spatial positive correlation and spatial clustering. Over the past 20 years, the spatial clustering of LER has weakened, and spatial autocorrelation has decreased, demonstrating the spatial changes and distribution characteristics of LER. (4) Water resources, NDVI, NPP, and distance to residence are key factors influencing the spatial distribution of LER. Among these, NDVI and NPP are the main driving factors for changes of LER. (5) Under three future development scenarios, the overall LER in the YRBD will continue to show a declining trend. The EPS scenario performs best in reducing LER, indicating that policies prioritizing ecological protection are most effective in reducing ecological risk. The changes in LER across different sub-regions under different development scenarios also exhibit heterogeneity, showing that a single development model cannot meet the needs for minimizing ecological risk in all sub-regions. Therefore, when formulating regional development plans, it is necessary to choose appropriate development paths based on the specific conditions of each sub-region, maximizing the balance of economic, social, and ecological factors to achieve the unity of ecological protection and economic development. This study provides comprehensive and scientific support for regional ecological protection and sustainable development and offers important references for ecological risk assessment and management in drylands worldwide.

Methods

Study area

The Yellow River originates from the Bayan Har Mountains in the northern part of the Tibetan Plateau and flows through nine provinces including Shandong, Henan, Shaanxi, Shanxi, Inner Mongolia, Ningxia, Gansu, Sichuan, and Qinghai, before emptying into the Bohai Sea. Its main stream is 5464 km long and covers a total area of 1.315 million km^2, involving 448 county-level administrative regions. According to the United Nations Convention to Combat Desertification (UNCCD), researchers such as Ci and Wu et al.[8,9] have used the Thornthwaite method for calculating the Moisture Index to divide the dryland zones of China, also known as potential extent of desertification in China. This delineation forms the basis for China's desertification monitoring research and serves as the standard range for the national desertification monitoring conducted every five years. Based on this delineation[68], the drylands of the Yellow River Basin (YRBD) include central and eastern Qinghai, eastern Gansu, Ningxia, central Inner Mongolia, and northern Shaanxi and Shanxi, involving 171 county-level administrative regions and accounting for 64% of the total area of the Yellow River Basin. The elevation in these areas ranges from 510 to 6130 m, covering major geomorphic units such as the TP, the LP, and the IMP (Fig. 8). Due to the west-high and east-low topographical pattern, there are significant climatic differences in the YRBD, with average annual temperatures ranging from −13.5 to 11.9 °C, and average annual rainfall varying from 7.9 to 897.7 mm. The population is mainly concentrated in the plains and river valleys, with agriculture and animal husbandry as the main economic activities. Industrial development is relatively low, primarily focused on resource extraction and primary processing. Due to the complex geomorphology, significant climate variability, and extensive human activities, The YRBD has heightened ecological vulnerability, leading to issues such as water scarcity, low ecological carrying capacity, and severe desertification. These challenges have become key areas of concern for ecological protection, high-quality development, and desertification control in the Yellow River Basin and across China.

Data collection

The LU data employed in this study in 2000, 2010 and 2020 were obtained from the China National Land Use/Cover Change (CNLUCC) dataset with resolution of 1 km (http://www.resdc.cn). Based on the actual conditions of the study region, the LU types were reclassified into 6 groups: grassland, forest, cropland, water, unused land, and built-up land. DEM were acquired from the Geographic Spatial Data Cloud (http://www.gscloud.cn) with a resolution of 30 m. The precipitation and temperature data at 1 km spatial resolution were retrieved from the National Earth System Science Data Center, National Science & Technology Infrastructure of China (http://www.geodata.cn). The population and GDP data were collected from the 1 km Grid Population Dataset of China and 1 km Grid GDP Data of China (http://www.resdc.cn), which are sourced from the Data Registration and Publishing System of Resource and Environment Science and Data Center. The nighttime light data were acquired from the China Long Term Nighttime Light Dataset[69], sourced from the Global Change Research Data Publishing & Repository (in both Chinese and English), with a spatial resolution of 1 km. The road, railway, urban, and river data were sourced from OpenStreetMap. The NPP and NDVI data were retrieved from the MODIS MOD17A3 and MOD13A3 data products (https://www.earthdata.nasa.gov), with spatial resolutions of 500 m and 1 km, respectively. The original data were processed by filling in missing values and synthesizing the maximum values. To ensure consistency in the analysis, all data underwent resampling to achieve a resolution of 1 km.

Research methods

Partitioning the region into ecological risk units

The utilization of risk cells as fundamental units for ecological risk assessment is an efficient and extensively employed approach in LER assessment. By considering the spatial heterogeneity of the landscape patterns, as well as the combined patch size and study region, a square cell measuring 20 km × 20 km was constructed using

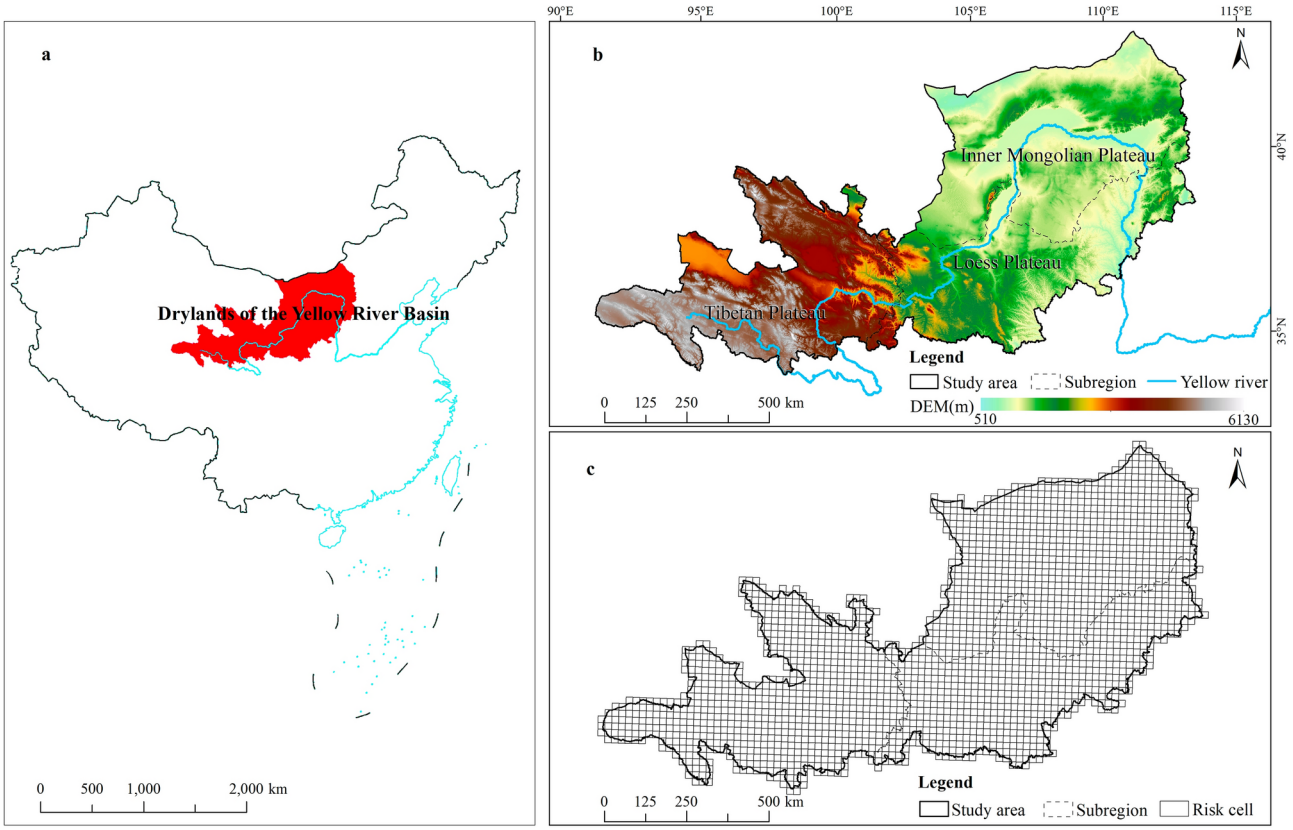

Fig. 8. Location of the YRBD (**a**, **b**) and LER assessment units of study area (**c**).

ArcGIS software for calculating the LER index (ERI). The YRBD was partitioned into 2334 ecological risk units, as depicted in Fig. 1c.

LER index

Based on existing literature[14,26,70,71], the ERI for the study area was constructed by selecting landscape dominance index, landscape isolation index, landscape fragmentation index, and landscape vulnerability index. This index quantitatively accesses the LER in risk units[72]. The following equation is used:

$$ERI_k = \sum_{i=1}^{n} \frac{A_{ki}}{A_k} L_i \tag{1}$$

where ERI_k represents the ERI of the *k*th risk unit, Aki denotes the area of the *i*th LU type within the kth risk unit, Ak indicates the total area of the kth risk unit, and L_i denotes the landscape loss index of the *i*th LU type.

The landscape loss index is defined as the degree of ecological loss of different landscapes under natural and human disturbance. It is thoroughly delineated by the landscape vulnerability index (V_i) and the landscape disturbance index (E_i). The following equation is used:

$$L_i = E_i \times V_i \tag{2}$$

The landscape disturbance index reflects the degree of interference of different landscapes by natural and human disturbances. It is defined using the landscape fragmentation index (F_i), landscape separation index (S_i), and landscape dominance index (D_i). The calculation formulas for specific indicators are presented in Table 6.

The vulnerability index reflects the susceptibility of different landscapes to external disturbances. Diverse LU types are regarded as different stages of natural landscape succession, and their vulnerability can be assigned according to prior studies[55,64]: unused land = 6, cropland = 5, grassland = 4, water = 3, forest = 2, and built-up land = 1. The values were obtained after normalization of 0.2857, 0.2381, 0.1905, 0.1429, 0.0952, and 0.0476 for the aforementioned LU types, respectively.

Based on the actual conditions and previous research, the natural breakpoint method was used to classify the ERI into five levels: High risk (ERI > 0.0448), Sub-high risk ($0.0306 < \text{ERI} \leq 0.0448$), Middle risk ($0.0218 < \text{ERI} \leq 0.0306$), Sub-low risk ($0.0164 < \text{ERI} \leq 0.0218$), and Low risk ($\text{ERI} \leq 0.0164$).

Index	Formula	Description
Landscape fragmentation (F_i)	$\mathrm{F_i} = \frac{\mathrm{n_i}}{\mathrm{A_i}}$	n_i denotes the patch count for the landscape i; A_i represents the total area of the landscape i
Landscape separation (S_i)	$\mathrm{S_i} = \frac{\mathrm{A}}{2\mathrm{A_i}}\sqrt{\frac{\mathrm{n_i}}{\mathrm{A}}}$	n_i denotes the patch count for the landscape i; A_i represents the total area of the landscape i; A indicates the total area
Landscape dominance (D_i)	$\mathrm{D_i} = \alpha \mathrm{L_i} + \beta \mathrm{M_i}$	Li denotes the ratio of the area for the landscape i and the total area for the study region; Mirepresents the ratio of the patch count for the landscape i and the total number for all patches; α and β indicate the weights of L_i and M_i (0.6 and 0.4, respectively)
Landscape disturbance (E_i)	$\mathrm{E_i} = \mathrm{aF_i} + \mathrm{bS_i} + \mathrm{cD_i}$	a, b, and c denotes the weights of F_i, S_i and D_i (0.5, 0.3 and 0.2, respectively)[25,28,73]

Table 6. Calculation of landscape ecological risk index.

Spatial autocorrelation analysis

Spatial autocorrelation analysis has been described at local and global levels[74]. Global spatial autocorrelation is employed to assess whether there is spatial autocorrelation in LER at a macro level within the study area, while local spatial autocorrelation is utilized to determine the presence of spatial autocorrelation within specific local regions within the study area at a micro level.

$$\mathrm{GMoran's}\ I = \frac{\sum_{i=1}^{m}\sum_{j=1}^{m} W_{ij}\left(x_i - \overline{x}\right)\left(x_j - \overline{x}\right)}{B^2 \sum_{i=1}^{m}\sum_{j=1}^{m} W_{ij}} \tag{3}$$

$$\mathrm{LMoran's}\ I = \frac{m\left(x_i - \overline{x}\right)\sum_{j=1}^{m} W_{ij}\left(x_j - \overline{x}\right)}{\sum_{i=1}^{m}\left(x_i - \overline{x}\right)^2} \tag{4}$$

where GMoran's I and LMoran's I are the global and local spatial autocorrelation index, respectively; m represents the total number of units; x_i and x_j denote the ERI value of unit i and adjacent unit j $(i \neq j)$, respectively; $\overline{x}$ is represents the average value of x; W_{ij} denotes the spatial weight matrix, and B indicates the variance of ERI value. The value of Moran's I range from -1 to 1. If $I > 0$, it signifies a positive spatial correlation, whereas a negative correlation is indicated if $I < 0$. If $I = 0$, there is no spatial correlation[75].

Identification of driving factors according to GDM

The Geographical Detector Model (GDM) was used to identify the factors influencing the spatio-temporal variation of LER[76–78]. Eleven geographical, socio-economic and ecological factors were selected as drivers, including distance to water, distance to residence, GDP, population density, DEM, relief degree of surface, annual mean precipitation, annual mean temperature, NPP, and NDVI. These factors were subjected to a classification process using the natural breakpoint method, and then quantitatively analyzed using the GDM. The ERI value was treated as the dependent variable, while the various factors were considered as independent variables. The influence of each factor on LER was measured using the q value. The following equation is used:

$$q = 1 - \frac{\sum_{h=1}^{L} N_h \sigma_h^2}{N\sigma^2} \tag{5}$$

where L denotes the number of categories; h indicates the driving factor layer ($h = 1, 2, \ldots; L$); Nh and N denote the number of units in layer h and the entire region, respectively; σ_h^2 and σ^2 indicate the variances in layer h and the entire region, respectively. The range of values for q is [0, 1], where a higher value signifies a more potent explanatory influence of the driving factor on LER.

Multi-scenario simulation through the PLUS model

The LU Prediction PLUS model was employed to simulate the LU patterns under multiple development scenarios for the year 2030. It is a raster-based patch-generated LU simulation model that can simulate the spatio-temporal dynamics of multiple LU types and determine the possible driving factors of LU changes[79]. It integrates two main modules: CA based on multi-type random patch seeds (CARS) and rule-mining framework based on a land expansion analysis strategy (LEAS), which have better explanatory power and higher accuracy for different LU changes[80]. The LEAS module extracts changes of LU types between two periods and explore the relationship between these changes and driving factors with the random forest algorithm. Then the growth probability for each LU type in the study area was calculated. The CARS module combines the growth probability, LU data, conversion matrix, and neighborhood weights of each LU type to simulates future LU patterns.

The equations for PLUS can be expressed as follows[79]:

$$P_{i,k}^{d}(x) = \frac{\sum_{n=1}^{M} I\left(h_n(x) = d\right)}{M} \tag{6}$$

$$OP_{i,k}^{d=1} = \begin{cases} P_{i,k}^{d=1} \times (r \times \mu_k) \times D_k^t \ if\ \Omega_{i,k}^t = 0 \ \ and \ \ r < P_{i,k}^{d=1} \\ P_{i,k}^{d=1} \times \Omega_{i,k}^t \times D_k^t \qquad\qquad\qquad all \ \ others \end{cases} \tag{7}$$

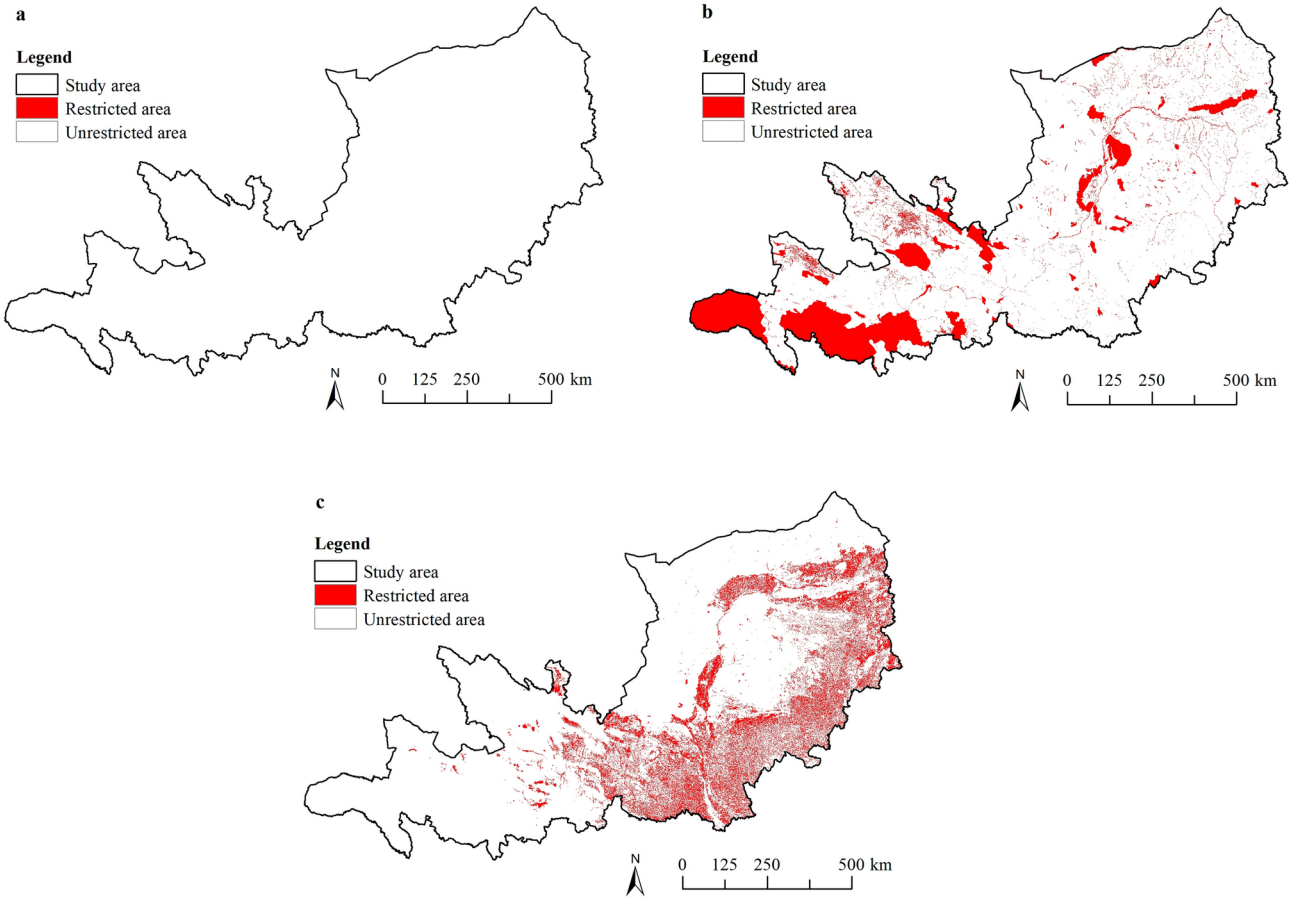

Fig. 9. The restricted area of Natural Development Scenario (NDS, **a**), Ecological Priority Scenario (EPS, **b**), Cropland Protection Scenario (CPS, **c**) in the study area (Software: ArcMap 10.6, http://www.esri.com).

where $P_{i,k}^{d}$ is the growth probability of LU type k at cell i; x is a vector composed of multiple driving factors; $I(\cdot)$ is the indicative function of the decision tree set; $h_n(x)$ is the prediction type of the n(th) decision tree for x; M is the total number of decision trees; the value of d is either 0 or 1; $OP_{i,k}^{d=1}$ is the overall probability of the LU type k; $P_{i,k}^{d=1}$ is the growth probability surface of LU type; r is a random number ranging from 0–1; μ_k is the threshold for LU type k to generate the new LU patches; D_k^t is a self-adaptive driving coefficient that relies on the difference between the current amount of land at iteration t and the target demand of LU k; $\Omega_{i,k}^t$ represents the neighborhood effects of cell i, which are the proportions of LU components of k within the surrounding neighborhood.

The LU patterns in 2020 were simulated based on the LU data from 2000 to 2010. The driving factors input into the PLUS model were the same as those used in the GDM. The figure of merit (FOM)[81,82] and overall accuracy (OA) were used to validate the accuracy of the simulation. According to the results, with FOM = 0.61 and OA = 0.97, the PLUS model achieved high simulation accuracy and can be employed to simulate the future LU patterns in the study area.

The study area encompasses two significant ecologically fragile regions: the Tibet Plateau and the "U-shape" area of Yellow River, which are key areas for ecological protection and restoration in China. Considering the various policies on cropland protection implemented since the third national land survey in China[83,84], we set three future development scenarios to simulate the LU and LER patterns in the YRBD in 2030: the Natural Development Scenario (NDS), the Ecological Priority Scenario (EPS) and the Cropland Protection Scenario (CPS). Under the NDS, the development trends of various land types from 2010 to 2020 continue without considering relevant policies and planning requirements, and no restrictions are imposed on the rules of LU type conversion. LU change occurs mainly due to the current socio-economic development status and ecogeographical factors. Under the EPS, based on the NDS, water bodies and national nature reserves within the study area are designated as ecological protection areas and set as restricted areas to prohibit LU transformations. Additionally, to protect the large areas of ecological land such as forest and grassland within the study area, the probability of transformation from grassland and forestland to unused land and built-up land is decreased by 20% and 50%, respectively. The EPS also considers cropland protection, and the probability of transformation from cropland to built-up land, a change induced by human activities, is decreased by 50%. Under the CPS, based on the NDS,

cropland is protected, and the transformation of cropland to other LU types is restricted. The restricted area is shown in Fig. 9.

The neighborhood weight of each LU type was determined by calculating the ratio of the expansion areas of a LU type accounting for the total land expansion based on the land expansion map[79]. According to the calculations, the neighborhood weights for cropland, forest, grassland, water, built-up land, and unused land were set to 0.20, 0.10, 0.41, 0.05, 0.9, and 0.44, respectively.

Data availability

All data generated or simulated in this study are available upon request to the corresponding author (lisshaxs@163.com). The land use, population and GDP data are available from http://www.resdc.cn. The DEM data are available from http://www.gscloud.cn. The precipitation and temperature data are available from http://www.geodata.cn. The nighttime light data are available from https://www.geodoi.ac.cn/edoi.aspx?DOI=https://doi.org/10.3974/geodb.2022.06.01.V1. The NDVI and NPP data are available from https://www.earthdata.nasa.gov.

Received: 4 March 2024; Accepted: 20 September 2024
Published online: 30 September 2024

References

1. Schulze, J., Frank, K. & Müller, B. Governmental response to climate risk: Model-based assessment of livestock supplementation in drylands. *Land Use Policy* **54**, 47–57 (2016).
2. Li, C. *et al.* Drivers and impacts of changes in China's drylands. *Nat. Rev. Earth Environ.* **2**, 858–873 (2021).
3. Berdugo, M. *et al.* Global ecosystem thresholds driven by aridity. *Science* **367**, 787–790 (2020).
4. Safaei, M. *et al.* Mapping terrestrial ecosystem health in drylands: Comparison of field-based information with remotely sensed data at watershed level. *Landsc. Ecol.* **38**, 705–724 (2023).
5. Wang, F. *et al.* Human-land coupling and sustainable human settlements in the Yellow River Basin. *Geogr. Res.* **39**, 1707–1724 (2020).
6. Zheng, Z., Lv, M. & Ma, Z. Climate, hydrology, and vegetation coverage changes in source region of Yellow River and countermeasures for challenges. *Bull. Chin. Acad. Sci.* **35**, 61–72 (2020).
7. Ewunetu, A., Simane, B., Teferi, E. & Zaitchik, B. F. Mapping and quantifying comprehensive land degradation status using spatial multicriteria evaluation technique in the headwaters area of upper blue Nile river. *Sustainability* **13**, 2244 (2021).
8. Wu, B., Su, Z. & Chen, Z. A revised potential extent of desertification in China. *J. Desert Res.* **27**, 911–917 (2007).
9. Ci, L. & Wu, B. Climatic type division and the potential extent determination of desertification of China. *J. Desert Res.* **17**, 107–111 (1997).
10. Sun, B. *et al.* Dynamic and dry/wet variation of climate in the potential extent of desertification in China during 1981–2010. *Environ. Earth Sci.* **73**, 3717–3729 (2015).
11. Sun, W. *et al.* Spatiotemporal vegetation cover variations associated with climate change and ecological restoration in the Loess Plateau. *Agric. For. Meteorol.* **209–210**, 87–99 (2015).
12. Huang, M.-T. & Zhai, P.-M. Desertification dynamics in China's drylands under climate change. *Adv. Clim. Change Res.* **14**, 429–436 (2023).
13. Wu, B. *et al.* Dynamics of land cover changes and driving forces in China's drylands since the 1970 s. *Land Use Policy* **140**, 107097 (2024).
14. Wang, H. *et al.* Spatial-temporal pattern analysis of landscape ecological risk assessment based on land use/land cover change in Baishuijiang National nature reserve in Gansu Province. *China. Ecol. Indic.* **124**, 107454 (2021).
15. Andow, D. A. & Hilbeck, A. Science-based risk assessment for nontarget effects of transgenic crops. *BioScience* **54**, 637–649 (2004).
16. Kim, Y. *et al.* Aquatic toxicity of acetaminophen, carbamazepine, cimetidine, diltiazem and six major sulfonamides, and their potential ecological risks in Korea. *Environ. Int.* **33**, 370–375 (2007).
17. Yi, Y., Yang, Z. & Zhang, S. Ecological risk assessment of heavy metals in sediment and human health risk assessment of heavy metals in fishes in the middle and lower reaches of the Yangtze River basin. *Environ. Pollut.* **159**, 2575–2585 (2011).
18. Shen, W., Zhang, J., Wang, K. & Zhang, Z. Identifying the spatio-temporal dynamics of regional ecological risk based on Google Earth Engine: A case study from Loess Plateau. *China. Sci. Total Environ.* **873**, 162346 (2023).
19. da Silva, R. F. B., Batistella, M. & Moran, E. F. Drivers of land change: Human-environment interactions and the Atlantic forest transition in the Paraíba Valley, Brazil. *Land Use Policy* **58**, 133–144 (2016).
20. Zeng, C., He, J., He, Q., Mao, Y. & Yu, B. Assessment of land use pattern and landscape ecological risk in the Chengdu–Chongqing economic circle, Southwestern China. *Land* **11**, 659 (2022).
21. Fu, J. *et al.* Ecological risk assessment of wetland vegetation under projected climate scenarios in the Sanjiang Plain, China. *J. Environ. Manag.* **273**, 111108 (2020).
22. Lin, X. & Wang, Z. Landscape ecological risk assessment and its driving factors of multi-mountainous city. *Ecol. Indic.* **146**, 109823 (2023).
23. Zhao, Z. & Zhang, T. Integration of ecosystem services into ecological risk assessment for implementation in ecosystem-based river management: A case study of the Yellow River, China. *Hum. Ecol. Risk Assess. Int. J.* **19**, 80–97 (2013).
24. Mörtberg, U. M., Balfors, B. & Knol, W. C. Landscape ecological assessment: A tool for integrating biodiversity issues in strategic environmental assessment and planning. *J. Environ. Manag.* **82**, 457–470 (2007).
25. Zhang, W., Chang, W. J., Zhu, Z. C. & Hui, Z. Landscape ecological risk assessment of Chinese coastal cities based on land use change. *Appl. Geogr.* **117**, 102174 (2020).
26. Xie, H., Wen, J., Chen, Q. & Wu, Q. Evaluating the landscape ecological risk based on GIS: A case-study in the Poyang Lake region of China. *Land Degrad. Dev.* **32**, 2762–2774 (2021).
27. Zhang, X. *et al.* Watershed landscape ecological risk assessment and landscape pattern optimization: Take Fujiang River Basin as an example. *Hum. Ecol. Risk Assess. Int. J.* **27**, 2254–2276 (2021).
28. Karimian, H., Zou, W., Chen, Y., Xia, J. & Wang, Z. Landscape ecological risk assessment and driving factor analysis in Dongjiang river watershed. *Chemosphere* **307**, 135835 (2022).
29. Wang, K. *et al.* Landscape ecological risk assessment of the Hailar River basin based on ecosystem services in China. *Ecol. Indic.* **147**, 109795 (2023).
30. Luo, F., Liu, Y., Peng, J. & Wu, J. Assessing urban landscape ecological risk through an adaptive cycle framework. *Landsc. Urban Plan.* **180**, 125–134 (2018).
31. Li, W., Wang, Y., Xie, S., Sun, R. & Cheng, X. Impacts of landscape multifunctionality change on landscape ecological risk in a megacity, China: A case study of Beijing. *Ecol. Indic.* **117**, 106681 (2020).
32. Gong, J. *et al.* Integrating ecosystem services and landscape ecological risk into adaptive management: Insights from a western mountain-basin area, China. *J. Environ. Manag.* **281**, 111817 (2021).

33. Wolfram, J., Stehle, S., Bub, S., Petschick, L. L. & Schulz, R. Water quality and ecological risks in European surface waters—Monitoring improves while water quality decreases. *Environ. Int.* **152**, 106479 (2021).
34. Xu, W., Wang, J., Zhang, M. & Li, S. Construction of landscape ecological network based on landscape ecological risk assessment in a large-scale opencast coal mine area. *J. Clean. Prod.* **286**, 125523 (2021).
35. Dong, S. *et al.* Synergetic prevention of desertification and green development in upper, middle and lower reaches of Yellow River Basin. *Environ. Sustain. Dev.* **46**, 44–49 (2021).
36. Li, J., Li, S., Zhang, Y. & Pang, J. Spatio-temporal variation of biodiversity maintenance function and its driving factors in the Yellow River Basin from 2000 to 2020. *China Environ. Sci.* **43**, 4780–4790 (2023).
37. Chi, W., Zhao, Y., Kuang, W. & He, H. Impacts of anthropogenic land use/cover changes on soil wind erosion in China. *Sci. Total Environ.* **668**, 204–215 (2019).
38. Wang, P., Wang, Y. J., Liu, X. P., Chen, X. & Kong, F. X. Ecological risk assessment of an ecological migrant resettlement region based on landscape structure: A case study of Hongsibu in Ningxia. *Acta Ecol. Sin.* **38**, 2672–2682 (2018).
39. Cheng, J., Wang, P., Chen, H. X. & Han, Y. G. Geographical exploration of the spatial and temporal evolution of ecological risk and its influencing factors in semi-arid regions: A case of Yanchi County in Ningxia. *Arid Land Geo.* **45**, 1637–1648 (2022).
40. Xu, B. *et al.* Landscape ecological risk assessment of Yulin Region in Shaanxi Province of China. *Environ. Earth Sci.* **81**, 1–14 (2022).
41. Gao, J. X. *et al.* Research on the method and application of large-scale ecological disturbance risk assessment. *China Environ. Sci.* **41**, 5274–5281 (2021).
42. Hu, B. *et al.* Stoichiometry of soil carbon, nitrogen, and phosphorus in farmland soils in southern China: Spatial pattern and related dominates. *CATENA* **217**, 106468 (2022).
43. Hao, J., Zhi, L., Li, X., Dong, S. & Li, W. Temporal and spatial variations and the relationships of land use pattern and ecosystem services in Qinghai–Tibet Plateau, China. *Chin. J. Appl. Ecol.* **34**, 3053–3063 (2023).
44. Dai, H. *et al.* Evaluation of the ecological benefits of main forest type in Inner Mongolian Daqing mountain. *J. Northwest A F Univ. (Nat. Sci. Ed.)* **39**(05), 98–102 (2011).
45. Liu, J. *et al.* Simulation of dynamic urban expansion under ecological constraints using a long short term memory network model and cellular automata. *Remote Sens.* **13**, 1499 (2021).
46. Wei, L., Zhou, D., Sun, D. & Tang, X. The evolution of spatio-temporal pattern and scenario simulation of urban agglomeration expansion in the Yellow River Basin: A case study in the Hohhot-Baotou-Ordos-Yulin Urban Agglomeration. *Geogr. Res.* **41**, 1610–1622 (2022).
47. Zhang, Y. *et al.* Spatial and temporal characteristics of land use and cover changes in the Tibetan Plateau. *Chin. Sci. Bull.* **64**, 2865–2875 (2019).
48. Shao, Q. & Liu, S. Assessment of ecological benefits of key national ecological projects in China in 2000–2019 using remote sensing. *Acta Geogr. Sin.* **77**, 2133–2153 (2022).
49. Fu, L. *et al.* Characteristics and driving forces of land use change in the Yellow River Basin from 2000 to 2020. *Ecol. Environ. Sci.* **31**, 1927–1938 (2022).
50. Liao, M. *et al.* Spatiotemoral characteristics of land use/coverage in the Yellow River Basin over the past 40y. *J. Soil Water Conserv.* **38**, 165–177+189 (2024).
51. Gao, J., Wang, Y., Hou, P. & Zhang, W. Temporal and spatial variation characteristics of land surface water area in the Yellow River Basin in recent 20 years. *J. Hydraul. Eng.* **51**, 1157–1164 (2020).
52. Ye, P. *et al.* Climate change in the upper Yellow River Basin and its impact on ecological vegetation and run-off from 1980 to 2018. *Trans. Atmos. Sci.* **43**, 967–979 (2020).
53. Liu, C., Li, X. & Jiang, D. Landscape pattern identification and ecological risk assessment using land-use change in the Yellow River Basin. *Trans. Chin. Soc. Agric. Eng.* **37**, 265–274 (2021).
54. Hua, Y., Chen, J., Sun, X. & Pei, Z. Analysis of landscape ecology risk of the Yellow River basin in Inner Mongolia. *Remote Sens. Nat. Resour.* **35**, 220–229 (2023).
55. Song, Q. *et al.* Spatio-temporal variation and dynamic scenario simulation of ecological risk in a typical artificial oasis in Northwestern China. *J. Clean. Prod.* **369**, 133302 (2022).
56. Qi, W. *et al.* Effects of ecological engineering on net primary production in the Chang Tang and Sanjiangyuan national nature reserves on the Tibetan Plateau. *Biodivers. Sci.* **24**, 127–135 (2016).
57. Wang, M. & Sun, X. Potential impact of land use change on ecosystem services in China. *Environ. Monit. Assess.* **188**, 248 (2016).
58. Zhou, W. *et al.* Grassland productivity increase was dominated by climate in Qinghai–Tibet Plateau from 1982 to 2020. *J. Clean. Prod.* **434**, 140144 (2024).
59. Wang, H., Yao, F., Zhu, H. & Zhao, Y. Spatiotemporal variation of vegetation coverage and its response to climate factors and human activities in arid and semi-arid areas: Case study of the Otindag Sandy Land in China. *Sustainability* **12**, 5214 (2020).
60. Deng, G. *et al.* Response of vegetation variation to climate change and human activities in semi-arid swamps. *Front. Plant Sci.* **13**, 990592 (2022).
61. Zhang, X. *et al.* Analysis on spatio-temporal evolution of ecological vulnerability in arid areas of Northwest. *Acta Ecol. Sin.* **41**, 4707–4719 (2021).
62. Zhu, Z., Mei, Z., Xu, X., Feng, Y. & Ren, G. Landscape ecological risk assessment based on land use change in the Yellow River Basin of Shaanxi, China. *Int. J. Environ. Res. Public. Health* **19**, 9547 (2022).
63. Wang, S., Tan, X. & Fan, F. Landscape Ecological risk assessment and impact factor analysis of the Qinghai–Tibetan plateau. *Remote Sens.* **14**, 4726 (2022).
64. Yang, L., Li, Y., Jia, L., Ji, Y. & Hu, G. Ecological risk assessment and ecological security pattern optimization in the middle reaches of the Yellow River based on ERI+MCR model. *J. Geogr. Sci.* **33**, 823–844 (2023).
65. Li, C. *et al.* Improved vegetation ecological quality of the three-north shelterbelt project region of China during 2000–2020 as evidenced from multiple remotely sensed indicators. *Remote Sens.* **14**, 5708 (2022).
66. Chen, X., Liu, C. & Yu, X. Urbanization, economic development, and ecological environment: Evidence from provincial panel data in China. *Sustainability* **14**, 1124 (2022).
67. Wang, D., Ji, X., Li, C. & Gong, Y. Spatiotemporal variations of landscape ecological risks in a resource-based city under transformation. *Sustainability* **13**, 5297 (2021).
68. China Desert Ecosystem Functions and Services Research Team. *Functions Assessment and Services Valuation of Desert Ecosystem in China* 2nd edn. (Science Press, 2016).
69. Zhong, X. Y., Yan, Q. W. & Li, G. Development of time series of nighttime light dataset of China (2000–2020). *J. Glob. Change Data Discov.* **6**, 416–424 (2022).
70. Ai, J. *et al.* Assessing the dynamic landscape ecological risk and its driving forces in an island city based on optimal spatial scales: Haitan Island. *China. Ecol. Indic.* **137**, 108771 (2022).
71. Liu, R. *et al.* Multi-scenario simulation of ecological risk assessment based on ecosystem service values in the Beijing–Tianjin–Hebei region. *Environ. Monit. Assess.* **194**, 434 (2022).
72. Qiao, B. *et al.* Ecological zoning identification and optimization strategies based on ecosystem service value and landscape ecological risk: Taking Qinghai area of Qilian Mountain National Park as an example. *Acta Ecol. Sin.* **43**, 986–1004 (2023).
73. Wang, B., Ding, M., Li, S., Liu, L. & Ai, J. Assessment of landscape ecological risk for a cross-border basin: A case study of the Koshi River Basin, central Himalayas. *Ecol. Indic.* **117**, 106621 (2020).

74. Ma, J., Ma, P., Li, C. X., Peng, Y. & Wei, H. Temporal and spatial variation of ecosystem service value in the three gorges reservoir region (Chongqing section) based on land use. *Sci. Silvae Sin.* **50**, 17–26 (2014).
75. Gao, B. *et al.* Multi-scenario prediction of landscape ecological risk in the Sichuan-Yunnan ecological barrier based on terrain gradients. *Land* **11**, 2079 (2022).
76. Wang, J. *et al.* Geographical detectors-based health risk assessment and its application in the neural tube defects study of the Heshun Region, China. *Int. J. Geogr. Inf. Sci.* **24**, 107–127 (2010).
77. Wang, J.-F., Zhang, T.-L. & Fu, B.-J. A measure of spatial stratified heterogeneity. *Ecol. Indic.* **67**, 250–256 (2016).
78. Chen, Y. *et al.* Spatiotemporal variations of surface ozone and its influencing factors across Tibet: A geodetector-based study. *Sci. Total Environ.* **813**, 152651 (2022).
79. Liang, X. *et al.* Understanding the drivers of sustainable land expansion using a patch-generating land use simulation (PLUS) model: A case study in Wuhan, China. *Comput. Environ. Urban Syst.* **85**, 101569 (2021).
80. Li, S. *et al.* Dynamic simulation of landscape ecological risk in mountain towns based on PLUS model. *J. Zhejiang Agric. For. Univ.* **39**, 84–94 (2022).
81. Varga, O. G., Pontius, R. G., Singh, S. K. & Szabó, S. Intensity analysis and the figure of merit's components for assessment of a cellular automata–Markov simulation model. *Ecol. Indic.* **101**, 933–942 (2019).
82. Tang, H. *et al.* Ecosystem service valuation and multi-scenario simulation in the Ebinur Lake basin using a coupled GMOP-PLUS model. *Sci. Rep.* **14**, 5071 (2024).
83. Lei, H., Zhu, P. & Hou, Y. Research on situation and problems of farmland protection in Qinghai-Tibet Plateau. *Nat. Resour. Inf.* 1–6. http://kns.cnki.net/kcms/detail/10.1798.n.20240513.1756.024.html (2024).
84. Xie, T. & Zhang, H. Land supply constraints, optimization of industrial land allocation and enterprise efficiency: Evidence from farmland protection policies. *Econ. Res. J.* **59**, 190–208 (2024).

Acknowledgements

This research was funded by the Basic Scientific Research Service Funds of Central Level Public Welfare Research Institutes, grant number CAFYBB2021ZB003.The authors would like to express their gratitude to EditSprings (https://www.editsprings.cn) for the expert linguistic services provided.

Author contributions

Conceptualization, J.L. and S.L.; Methodology, J.L. and S.L.; Data curation, X.W.; Formal analysis, J.L.; Resources, S.L.; Visualization, S.L., G.X., and J.P.; Writing-original draft, J.L.; Writing-review & editing, J.L., S.L., X.W., G.X. and J.P. All authors have read and agreed to the published version of the manuscript.

Competing interests

The authors declare no competing interests.

Additional information

Correspondence and requests for materials should be addressed to S.L.

Reprints and permissions information is available at www.nature.com/reprints.

Publisher's note Springer Nature remains neutral with regard to jurisdictional claims in published maps and institutional affiliations.